

Evaluation of Fatigue Damage in 304 Stainless Steel by Measuring Residual Magnetic Field

Yi LIU^a, Xiwang LAN^a and Bo HU^{a,1}

^a*Key Laboratory of Nondestructive Testing, Ministry of Education, Nanchang Hangkong University, Nanchang, PR China*

Abstract. To demonstrate the feasibility of the passive magnetic NDT method for damage assessment of 304 austenitic stainless steel, the residual magnetic field change of the 304 stainless steel specimens under fatigue loads was investigated. The measurement was carried out using a fluxgate sensor and the magnetic characteristics were extracted for analysis of fatigue state. Then, the XRD test was carried out to investigate the mechanism of magnetic field changes and verify the reliability of the proposed method. The results show that the variation of the maximum gradient is consistent with the process of fatigue crack growth, which indicates that the fatigue damage can be estimated by residual magnetic field measuring. In future stage, how to distinguish the magnetic field changes derived from martensite transformation or stress magnetization effect will be investigated.

Keywords. 304 stainless steel, residual magnetic field, fatigue damage, martensite transformation

1. Introduction

Damage assessment is a significant part of Materials' State Awareness (MSA) and Non-destructive Evaluation (NDE) technologies [1]. At present, several different electromagnetic NDE methods for damage assessment such as Magnetic Barkhausen Noise (MBN), Pulsed Eddy Current (PEC), magnetic properties measurement, and Potential Drop (PD) detection have been proposed. MBA method is an active magnetic technique usually in need of high strength, low-frequency fields to drive the material into saturation [2]. PEC testing has a limited sensitivity in depth owing to skin effect [3]. Passive magnetic NDT methods such as Metal Magnetic Memory (MMM) or Residual Magnetic Field (RMF) measurement, have been widely verified in the damage assessment of ferromagnetic materials [2,4]. However, 304 austenitic stainless steel is a paramagnetic material with low permeability (about 2~3 orders of magnitude lower than ferromagnetic materials), and the induction magnetic field variations caused by stress or fatigue is small. Therefore, they put forward higher requirements for sensor sensitivity compared with ferromagnetic materials. PD method has been exploited for creep monitoring of nonferromagnetic materials such as SUS 304 austenitic stainless steel and aluminum alloy [5]. However, the sensitivity to creep is low in the absence of geometrical effect of deformation [6]. Considering the low permeability of 304 stainless

¹ Corresponding Author, Bo HU, Tel.: +86 13627914320; E-mail: cumthubo@163.com.

Figure 1. Schematic diagram of sample geometry.

2.2. Experimental Setup and Procedure

The experiment was carried out in three processes. During the first stage, a magnetization test was performed to determine the initial magnetization state of 304 stainless steel. The base metal was processed into small pieces of $2\text{ mm} \times 2\text{ mm} \times 2\text{ mm}$ as test samples by wire-electrode cutting. After being polished, the samples were put into an ultrasonic oscillator and cleaned with distilled water and then being dried. A comprehensive physical property measurement system (SQUID) produced by the Quantum Design company of the United States was used. The test temperature was 300 K, and the maximum applied magnetic field was 2 T.

Then, an Instron8801 electronic universal testing machine was used to perform a tensile–tensile fatigue test of 304 stainless steel. The main parameters load, stress ratio, and the maximum loading frequency were set as 230 MPa, 0.1, and 10 Hz respectively. After every certain loading cycle, the residual magnetic field of the specimen was measured by a magnetic probe composed of a fluxgate sensor. The magnetic core material of the sensor was cobalt-based amorphous alloy, which has high permeability and low coercivity ensuring good anti-interference effect and low loss [7]. The measurement range was $10^{-10}\text{ T} \sim 10^{-4}\text{ T}$, the resolution was 0.1 nT, the measurement error was $\pm 0.25\%$, the measurement frequency and the detection distance was set as 25 Hz and 60 mm respectively. The specimen was detected in a stable magnetic field environment with the probe vertical to the sample surface and without lift-off. The experimental setup is shown in Figure 2.

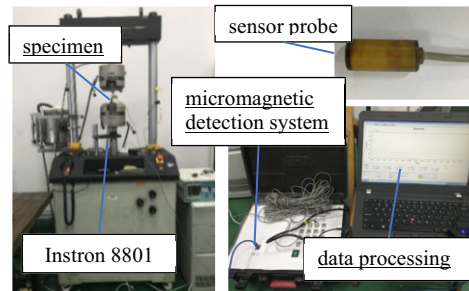


Figure 2. Photo of the experimental setup.

Finally, to verify the martensitic transformation of 304 stainless steel in the fatigue process, the X-ray diffraction test was conducted on the specimens before and after fatigue. The samples were processed into small blocks of $10\text{ mm} \times 10\text{ mm} \times 3\text{ mm}$. As in the first stage, the block samples were mechanically polished and then cleaned before use. A D8 Advance X-ray diffractometer was used to conduct phase analysis in this test. The incident wavelength was 1.5406 \AA , the measuring angle range was $20^\circ \sim 80^\circ$, the step length was 0.02° , and the measuring temperature was 300 K.

3. Results and Discussion

3.1. Initial Magnetism of 304 Stainless Steel

Figure 3(a) shows the magnetization curve of 304 stainless steel. As can be seen, the magnetization of the material is approximately linear with the increase in the external

magnetic field, and there is no magnetic saturation. Additionally, the magnetization curve has weak hysteresis near the zero magnetic field. The magnetic susceptibility is calculated, which is shown in Figure 3(b). When the external magnetic field is within ± 6000 A/m, the magnetic susceptibility of sample 1 is between 0.022–0.243, and that of sample 2 is between 0.046–0.303. As a result, the average relative magnetic permeability is between 1.034–1.273, which is 2–3 orders of magnitude lower than that of ferromagnetic materials. Therefore, the initial state of 304 stainless steel is paramagnetic.

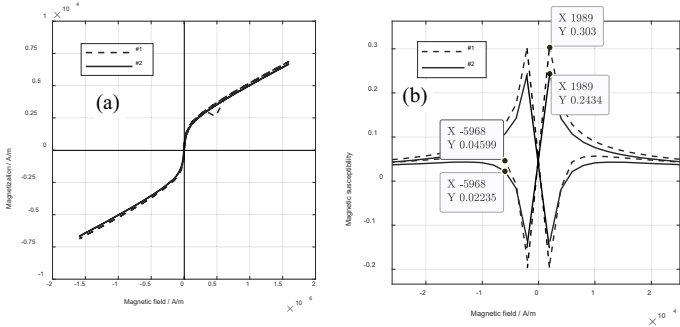


Figure 3. H–M curve (a) and susceptibility curve (b).

3.2. Variations of Magnetic Induction Intensity and Magnetic Gradient

Figure 4 shows the magnetic induction field of 304 stainless steel under different cyclic loads. It can be seen that the initial magnetic induction intensity on both sides is greater than that at the center. With the increase in cycles, the magnetic field curve rotates clockwise and when the cycles reach 42048, the specimen breaks and the curve fluctuates sharply. This indicates that the induction magnetic field is sensitive to component fracture, but it cannot characterize the early fatigue damage as the variations of 100–10,000 cycles are not significant. It is noted that there is no magnetic field data from 10,000 to 42,048 cycles, this is because the effect of residual stress on fatigue life was underestimated in the experiment. Generally, the fatigue cycle of 304 stainless steel in a low-stress area ($< (0.3\sim 0.45)\sigma_b$) can reach 100,000 times [8]. But in this test, the specimen was taken off from the fatigue machine after a certain cycle to measure the magnetic field, and then reloaded. This resulted in the addition of residual stress to the applied load, and caused low cycle fatigue of the specimen.

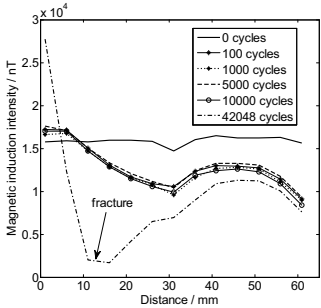


Figure 4. Magnetic induction intensity under different cycles.

To further describe the variations of the residual magnetic field, the gradient was extracted to be investigated. It can be expressed as: $k_B = \frac{dB}{dx}$, where k_B is the magnetic

gradient, B represents the induction magnetic field, and x denotes the measurement distance. Figure 5(a) shows the gradient signal without fatigue. The magnetic gradient has a peak value at the center of the sample, which is opposite to the magnetic field change trend showed in Figure 4. Therefore, it is believed that gradient k_B can only qualitatively reflect the stress concentration but cannot quantitatively represent the magnitude of stress or fatigue damage. Multiple methods should be used to further investigate the correlation between gradient k_B and fatigue degree.

The k_{Bmax} is the maximum magnetic gradient in a scanning process, and it usually appears around cracks and is considered to have some correlation with crack depth [9]. The gradient k_{Bmax} under different cycles is calculated, as presented in Figure 5(b). k_{Bmax} increases slowly with the increasing loading cycles in the early and middle stages and increase sharply in late stage. By the least square method, the fitting result can be expressed as $y = 0.0038 \times x + 3.5e^2$. According to the theory of fatigue crack growth [8], it can be seen that the variation trend of k_{Bmax} is the same as that of crack depth with the increase of loading cycles in the fatigue process. From the results, it should be underlined that there is a certain rule between the maximum gradient and fatigue damage. However, further research should be done considering the various factors that affect magnetic such as the material, temperature, and geometry of the specimen.

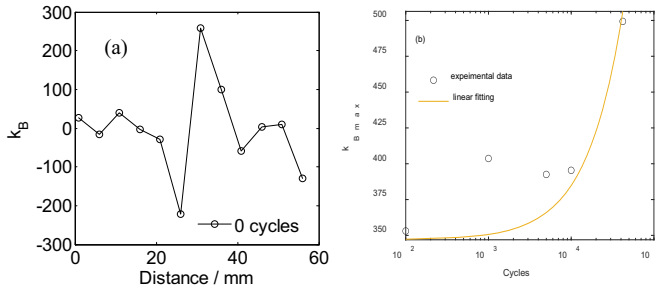


Figure 5. Variations of magnetic characteristic parameters with cycles:

(a) magnetic gradient k_B , (b) maximum gradient k_{Bmax} .

3.3. XRD Analysis

Figure 6 shows the XRD diffraction intensity spectrum of the 304 stainless steel samples before fatigue and after a fracture. For the sample after fatigue, the diffraction peaks of α' martensite phase is superimposed on that of the original γ austenite phase and the highest peak $\gamma(111)$ decreases largely, whereas the $\alpha'(110)$ increases relatively. Therefore, we can conclude that fatigue has caused the martensite transformation and changed the magnetic permeability as well as the residual magnetic field of 304 stainless steel. However, there are several challenges to characterize the fatigue damage of austenitic stainless steel by the residual magnetic field measurement. First, the martensite transformation is strongly temperature-dependent, which increases the uncertainty of sensitivity for components working at high temperature. Second, the transformation is a significant factor affecting magnetism but is not directly related to the life reduction. Furthermore, the magnetic sensor might be sensitive to other factors such as stress magnetization and surface morphology simultaneously, which might cause the lack of selectivity for the particular fatigue damage.

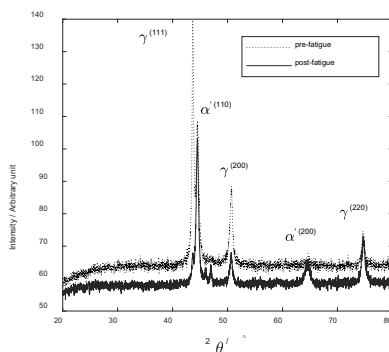


Figure 6. XRD spectrum of 304 stainless steel samples before and after fatigue.

4. Conclusions

This paper presented a residual magnetic field measurement method based on the fluxgate sensor for the evaluation of fatigue damage in paramagnetic 304 stainless steel. It was found that the maximum magnetic gradient increases with the increase in fatigue cycles and the variation rules are consistent with the law of crack growth in the fatigue process. The martensitic transformation caused by fatigue might be the main reason for the change of the residual magnetic field. It is possible to estimate fatigue damage of 304 stainless steel components by the passive magnetic NDT method. Future research will include demonstrating the feasibility of passive magnetic DNT methods in damage assessment of austenitic stainless steel under high temperature. The selectivity of detection methods for particular materials and damage mechanism types will be investigated. Additionally, the multi-modal monitoring in combination with other methods will be developed for comprehensive evaluation of material states in practical engineering situation.

References

- [1] P. B. Nagy, Non-destructive methods for materials' state awareness monitoring, *Insight* **52** (2010), 61–71.
- [2] J. W. Wilson, G.Y. Tian, S. Barrans, Residual magnetic field sensing for stress measurement, *Sensors and Actuators A: Physical* **135** (2007), 381–387.
- [3] M. Morozov, G.Y. Tian, P. J. Withers, Elastic and plastic strain effects on eddy current response of aluminium alloys, *Nondestructive Testing and Evaluation* **28** (2013), 300–312.
- [4] N. Venkatachalapathi, G.J. Raju, P. Raghavulu, Characterization of fatigued steel states with metal magnetic memory method, *Materials Today: Proceedings* **5** (2018): 8645–8654.
- [5] G. Sposito, C. Wardab, P. Cawley, et al, A review of non-destructive techniques for the detection of creep damage in power plant steels, *Ndt & E International* **43** (2010), 555–567.
- [6] E. Madhi, P. B. Nagy, Sensitivity analysis of a directional potential drop sensor for creep monitoring, *Ndt & E International* **44** (2011), 708–717.
- [7] L.J. Yang, C.B. Tu, S.W. Gao, Detection method of weak magnetic field based on fluxgate sensor, *Instrument Technique and Sensor* **09** (2014), 84–87.
- [8] R.T. Liu, W. B. Liu, J.Y. Liu, Mechanical properties of engineering materials, Harbin Institute of Technology, Harbin, 2001.
- [9] N. Chen, H. Lin, X.K. Wang, Crack propagation analysis and fatigue life prediction for structural alloy steel based on metal magnetic memory testing, *Journal of Magnetism and Magnetic Materials* **462** (2018), 144–152.